BBA - Molecular Basis of Disease 1865 (2019) 2563–2575

Contents lists available at ScienceDirect

BBA - Molecular Basis of Disease

journal homepage: www.elsevier.com/locate/bbadis

Protein arginine methyltranferase-1 induces ER stress and epithelial-mesenchymal transition in renal tubular epithelial cells and contributes to diabetic nephropathy

Yin-Yin Chen[a], Xiao-Fei Peng[b], Guo-Yong Liu[c], Jin-Song Liu[d], Lin Sun[e], Hong Liu[e], Li Xiao[e], Li-Yu He[e,*]

[a] Department of Nephrology, Laboratory of Kidney Disease of Hunan Provincial People's Hospital, Hunan Normal University, Changsha 410005, PR China
[b] Department of Rheumatology and Immunology, The Second Xiangya Hospital, Central South University, Changsha 410011, PR China
[c] Department of Nephrology, The First Affiliated Hospital of Changde Vocational Technical College, Changde 415000, PR China
[d] Department of Nephrology, Chinese Medicine and Western Medicine Hospital Affiliated to Hunan University of Chinese Medicine, Changsha 410011, PR China
[e] Department of Nephrology, The Second Xiangya Hospital, Central South University, Changsha 410011, PR China

ARTICLE INFO

Keywords:
Diabetic nephropathy
PRMT1
ER stress
Epithelial-mesenchymal transition
Fibrosis

ABSTRACT

Background: In this study, we examined the association of PRMT1 with ER stress and epithelial-mesenchymal transition (EMT), two critical pathogenic mechanisms leading to DN development, in proximal tubular epithelial cells (PTECs).

Methods: The level of PRMT1 was compared between the serum from DN patients and healthy individuals by ELISA, and between renal tissues of DN mice and normal mice using RT-qPCR and immunohistochemistry. Using high-glucose-treated PTEC cell line, HK2 cells as the model system, the significance of PRMT1 in ER stress and EMT was assessed by shRNA targeting PRMT1 (sh-PRMT1) and/or by overexpressing PRMT1. Mechanistic studies focused on three major pathways controlling ER stress: protein kinase R-like ER kinase (PERK), inositol requiring-1α (IRE1α), and activating transcription factor 6 (ATF6).

Results: PRMT1 was up-regulated in the serum of DN patients and renal tissues of DN mice. High glucose administration induced elevation of PRMT1 expression in HK2 cells *in vitro*, accompanied with ER stress and EMT activation. PRMT1 knockdown attenuated high glucose-induced ER stress and apoptosis by inactivating PERK and ATF6, but not IRE1α. PRMT1 activated ATF6 by recruiting H4R3me2as to the promoter. Furthermore, PRMT1-induced ER stress was concomitant with the activation of an EMT-like state. Specifically, inhibition of ATF6, but not PERK blocked PRMT1-induced EMT in high-glucose-treatment HK2 cells.

Conclusions: By activating ER stress, PRMT1 essentially regulates the apoptosis and EMT of PTECs in response to diabetic milieu. Thus, targeting PRMT1 may alleviate both tissue injury and renal fibrosis, and thus benefit the treatment of DN.

1. Introduction

Diabetic nephropathy (DN) is the life-threatening renal complication of increasingly prevalent diabetes and has become the major cause of end-stage renal failure [1,2]. Between 20% and 40% of all diabetic patients will develop DN worldwide [3]. The pathological lesions associated with DN development involve glomerular, interstitial, and vascular compartments [4], and are characterized by tissue injury associated with the excessive depositions of extracellular matrix (ECM) proteins, such as collagens, fibronectin, and laminin, which leads glomerulosclerosis, tubulointerstitial fibrosis, and renal fibrosis [5]. Understanding the mechanisms underlying the pathological changes of DN will help to develop effective therapies targeting this pandemic disease.

As a major cell type responsible for producing ECM components, the myofibroblasts positive for alpha smooth muscle actin (α-SMA) are found to be activated and their number inversely correlated with renal functions in DN patients [6]. A key mechanism leading to the activation and abundance of myofibroblasts in DN is epithelial-mesenchymal transition (EMT), by which the renal tubular epithelial cells lost the

* Corresponding author at: Department of Nephrology, The Second Xiangya Hospital, Central South University, Key Laboratory of Kidney Disease and Blood Purification in Hunan, No.139, Renmin Road, Changsha 410011, Hunan Province, PR China.
E-mail address: heliyu1124@csu.edu.cn (L.-Y. He).

https://doi.org/10.1016/j.bbadis.2019.06.001
Received 6 November 2018; Received in revised form 27 May 2019; Accepted 3 June 2019
Available online 11 June 2019
0925-4439/

epithelial features, as represented by the reduced expressions of epithelial markers such as E-cadherin and β-catenin, and obtained the mesenchymal features, as manifested by the enhanced expressions of myofibroblast markers including α-SMA and fibronectin [7]. It is reported that up to 36% of myofibroblasts may arise from tubular epithelial cells by EMT during renal fibrosis [8]. In spite of the significance of EMT in DN development, little is known on the molecular mechanisms controlling EMT in renal tubular epithelial cells, although diabetes-associated stress signals, such as hyperglycemia, oxidative stress, and advanced glycation end-products (AGEs), are suggested to induce EMT in podocytes and to contribute to DN development [9]. In addition to inducing EMT, diabetic milieu also triggers unfolded protein response (UPR) and activates endoplasmic reticulum (ER) stress [10]. During ER stress, the ER chaperone protein glucose-regulated protein 78 (GRP78) dissociates from the three major ER sensors, namely protein kinase R-like ER kinase (PERK), inositol requiring-1α (IRE1α), and activating transcription factor 6 (ATF6), leading to the activation/phosphorylation of the former two and the cleavage of ATF6, resulting in the phosphorylation of eukaryotic translation initiation factor-2α (eIF2α) and the expression of UPR targets such as ATF4 and C/EBP homologous protein (CHOP) [10]. Recent studies suggest that ER stress may crosstalk with EMT in distinct cell types [11–13], yet little is known whether these two processes interact during DN development.

Protein arginine methyltranferase-1 (PRMT1), a member in the PRMT family, is the primary enzyme responsible for the post-translational asymmetric dimethylation of arginine residues of both histone and non-histone proteins [14]. Functionally, PRMT1 controls the expression of a variety of substrate genes and regulates a repertoire of biological processes during normal physiology as well as pathological developments. Several recent studies suggest that PRMT1 expression is up-regulated in different compartments of DN tissues, including proximal tubular epithelial cells (PTECs), mesangial cells, and podocytes, and is functionally detrimental to each compartment [15–17]. Specifically, PRMT1 activates ER stress and induces apoptosis of mesangial cells [16]. In multiple cancer models, PRMT1 presented activities in modulating EMT and promoting cancer malignancy [18–20]. It is not known, however, whether activating ER stress and/or inducing EMT are integral for the disease-promoting activities of PRMT1 during DN development.

To answer these questions, we measured PRMT1 level from the serum of DN patients as well as in renal tissues from a streptozotocin (STZ)-induced mouse DN model. Then we focused on a PTEC cell line, HK2 cells and examined the potential involvement of PRMT1 in ER stress and EMT in high-glucose-challenged HK2 cells, and the underlying signaling mechanisms linking these two processes. This study reveals, for the first time, that PRMT1 critically controls ER stress in HK2 cells in response to diabetic milieu, which in turn induces EMT of these cells and contributes to renal fibrosis and DN development.

2. Materials and methods

2.1. Human samples and mouse tissues

This study was approved by the Ethics Committee and the Institutional Animal Care and Use Committee of The Second Xiangya Hospital, Central South University. Tissue specimens (diabetic nephropathy, $n = 10$ and control, $n = 3$) were obtained from patients at the Second Xiangya Hospital, between 2016 and 2017 and fixed in 10% formaldehyde. Resume specimens were obtained from thirty DN patients and thirty healthy individuals and written consent was obtained from each participant. Upon overnight fasting, peripheral blood was collected, allowed to clot at room temperature for 30 min, centrifuged at 2000 $\times g$ for 10 min, and the serum supernatant was transferred into a clean tube. The serum levels of PRMT1 were measured using the human PRMT1 ELISA kit (Abbexa, Cambridge, UK) according to the manufacturer's instructions.

To establish the mouse DN model, mice (C57, 4-week, Shanghai Super–B&K Laboratory Animal Corporation in China) were intraperitoneally injected with STZ (Sigma-Aldrich, St. Louis, MO, USA) prepared in sodium citrate buffer at 45 mg/kg body weight for five consecutive days. Those injected with equal volumes of sodium citrate buffer (vehicle) on the same schedule were used as control ($n = 6$). The mice in STZ group (n = 6) were measured for body weight and blood glucose level every three days thereafter. At one week after STZ injection, mice presenting a fasting blood glucose level of ≥280 mg/dL were considered successful for DN modeling and included in this study. At 5 time after STZ injection, all mice were sacrificed, with renal tissue isolated for further analysis.

2.2. Hematoxylin and eosin (HE) and periodic acid-Schiff methenamine silver methenamine (PASM) staining

Renal tissues from control and DN mice were fixed in formaldehyde, embedded in paraffin, and prepared into 4-μm sections. For general morphological assessment, the tissues were stained using HE staining kit (Vector Laboratories, Burlingame, CA, USA) following the manufacturer's instructions. For PASM staining, tissue sections were deparaffinized in xylene and rehydrated in a series of diluted alcohol. Upon washing in distilled water, tissue sections were stained using PASM staining kit (Polysciences, Warrington, PA, USA) according to manufacturer's protocol. All histological sections were imaged under a Nikon Eclipse Ci light microscope (Nikon, Tokyo, Japan).

2.3. Cell culture and treatments

The human PTECs HK2 cells were purchased from the American Type Culture Collection (Manassas, VA, USA) and cultured in Keratinocyte Serum Free Medium (Gibco, Carlsbad, CA, USA) supplemented with 0.05 mg/mL bovine pituitary extract and 5 ng/mL human recombinant epidermal growth factor (Gibco) at 37 °C in humidified atmosphere of 5% CO_2.

For treatment with high glucose and/or inhibitors, HK2 cells (including those stably expressing shRNAs or PRMT1, as described below) were treated with 1 μM GSK2606414 (specific PERK inhibitor; Millipore, Billerica, MA, USA), or 100 μM AEBSF (specific inhibitor for ATF6 cleavage; Sigma-Aldrich) in serum-free medium for 30 min, followed by high glucose [21,22] (30 mM; Sigma-Aldrich) or isotonic mannitol (5%; Sigma-Aldrich) for a further 48 h, and repeat operation for future 1–2 weeks.

2.4. Construction and transduction of lentiviruses knocking down or overexpressing PRMT1

To stably knock down the endogenous expression of PRMT1 in HK2 cells, shRNA specifically targeting PRMT1 (sh-PRMT1: sense, 5′-CACC GGACATGACATCCAAAGATTTCAAGAGAATCTTTGGATGTCATGTCTT TTTTG-3′; antisense, 5′-GATCCAAAAAAGACATGACATCCAAAGATTC TCTTGAAATCTTTGGATGTCATGTCC-3′) or negative control shRNA (sh-NC: sense, 5′-CACCGTTCTCCGAACGTGTCACGTCAAGAGATTACG TGACACGTTCGGAGAATTTTTTG-3′; antisense, 5′-GATCCAAAAAAGT TCTCCGCGTGTCACGTAATCTCTTGACGTGACACGTTCGGAGAAC-3′) were cloned into lentiviral vector pGLV2-U6-puro (GenePharma, Shanghai, China). To overexpress PRMT1 in HK2 cells, PRMT1 cDNA was cloned into lentiviral vector pHBLV, empty vector was used as the negative control. To generate lentivirus, lentiviral and packaging vectors were co-transfected into 293T cells. At 48 h after the transfection, the supernatant containing lentivirus was collected and centrifuged at 500 $\times g$ for 5 min to remove any cell debris. For lentiviral transduction, HK2 cells were incubated with lentivirus in the presence of polybrene (8 μg/mL; Sigma-Aldrich) overnight. Then the cells were cultured in fresh complete growth medium for 48 h or a further two weeks.

2.5. Immunohistochemistry and immunofluorescence

To examine the expressions of PRMT1, GRP78, and CHOP, renal tissue sections from control or DN mice were deparaffinized, rehydrated, and antigen retrieved using citric acid-based antigen unmasking solution (Vector Laboratories) according to the manufacturer's instructions. After blocking in Animal-Free Blocker (Vector Laboratories), tissue sections were incubated with anti-PRMT1 (ab73246; Abcam, Cambridge, MA, USA), anti-GRP78 (ab21685; Abcam), or anti-CHOP (MA1-250; Invitrogen) antibody at 4 °C overnight. The next morning, tissue sections were incubated with HRP-conjugated secondary antibody at room temperature for 30 min, washed, and the signal was developed using DAB Plus Substrate System (Thermo Fisher Scientific) according to the manufacturer's instructions. After counterstaining with hematoxylin (Vector Laboratories) at room temperature for 5 min, slides were rinsed with running tap water, dried, and mounted with permanent mounting media (Vector Laboratories).

For immunofluorescence, HK2 cells upon indicated treatments were washed three times in PBS and fixed with 4% paraformaldehyde at room temperature for 10 min. After three washes in PBS, cells were permeabilized with 0.2% Triton X-100, blocked in 1% bovine serum albumin (BSA) solution, and incubated with anti-PRMT1, anti-GRP78, anti-CHOP, anti-E-cadherin (#680181; BD Biosciences, San Jose, CA, USA), anti-β-catenin (#610154, BD Biosciences), anti-ZEB1 (ab155249, Abcam), anti-ZO-1 (ab221547, Abcam), anti-fibronectin (#610077, BD Biosciences), or anti-α-SMA (#A5228, Sigma-Aldrich) antibody at 4 °C overnight. After three washes in PBS, the cells were incubated with Alexa Fluor 488 or 594 labeled secondary antibody (Sigma-Aldrich). Then the cells were mounted on slides using the ProLong Gold Antifade Mounting Medium (Invitrogen) containing the nuclear stain 4′, 6-diamidino-2-phenylindole (DAPI).

2.6. Extraction of total RNA and quantitative real-time PCR (RT-qPCR)

Total RNA was extracted from tissues or HK2 cells using Trizol reagent (Invitrogen) according to the manufacturer's instructions. cDNA was then synthesized using oligo dT as the primer with AMV reverse transcriptase (Invitrogen). RT-PCR was performed in the ABI PRISM 7300 Fast Real-Time PCR System (Ambion, Austin, TX, USA) using the following primers: mouse Prmt1 forward 5′-CTGCCTCTTCTACGAGTC CATG-3′ and reverse 5′-TCGGTCCTCAATGGCTGTCACA-3′; human PRMT1 forward 5′-TGCGGTGAAGATCGTCAAAGCC-3′ and reverse 5′-GGACTCGTAGAAGAGGCAGTAG-3′; human GRP78 forward 5′-CTG TCCAGGCTGGTGTGCTCT-3′ and reverse 5′-CTTGGTAGGCACCACTGT GTTC-3′; human CHOP forward 5′-GGTATGAGGACCTGCAAGAGGT-3′ and reverse 5′-CTTGTGACCTCTGCTGGTTCTG-3′; human ATF6 forward 5′-GTTCTTCCGTCAACTCTGAGGC-3′ and reverse 5′-GGACTCTGTCTT CACTTCCAGG-3′; human E-cadherin forward 5′-GCCTCCTGAAAAGA GAGTGGAAG-3′ and reverse 5′-TGGCAGTGTCTCTCCAAATCCG-3′, human β-catenin forward 5′-CACAAGCAGAGTGCTGAAGGTG-3′ and reverse 5′-GATTCCTGAGAGTCCAAAGACAG-3′; human fibronectin forward 5′-ACAACACCGAGGTGACTGAGAC-3′ and reverse 5′-GGACA CAACGATGCTTCCTGAG-3′; human α-SMA forward 5′-AAGAGGAATC CTGACCCTGAA-3′ and reverse 5′-TGGTGATGATGCCATGTTCT-3′; and GAPDH (internal control) forward 5′-GTCTCCTCTGACTTCAACA GCG-3′ and reverse 5′-ACCACCCTGTTGCTGTAGCCAA-3′. Each reaction was set up in triplicate and the relative expression level of a target gene was calculated as a ratio to that of the internal control using $2^{-\Delta\Delta Ct}$ method [23].

2.7. Western blot

The tissues or HK2 were collected and lysed using cell lysis buffer (Beyotime, China). Equal amount of total proteins from each sample were separated on SDS-PAGE gel, and blotted onto a polyvinylidene difluoride membrane. The target protein was probed with one of the following primary antibodies at 4 °C overnight: anti-PRMT1 (ab73246, Abcam), anti-GRP78 (ab21685, Abcam), anti-CHOP (MA1-250, Invitrogen), anti-ATF6 (ab11909, Abcam), anti-p-PERK (sc-32577-R, Santa Cruz Biotechnology, Santa Cruz, CA, USA), anti-p-eIF2α (#9721; Cell Signaling Technology, Danvers, MA, USA), anti-p-IRE (ab48187, Abcam), anti-E-cadherin (#680181; BD Biosciences), anti-β-catenin (#610154, BD Biosciences), anti-ZEB1 (ab155249, Abcam), anti-ZO-1 (ab221547, Abcam), anti-fibronectin (#610077, BD Biosciences), anti-α-SMA (#A5228, Sigma-Aldrich), or anti-β-actin (internal control; #A1978, Sigma-Aldrich). After the incubation with horseradish peroxidase-conjugated secondary antibodies at room temperature for 2 h. The signal was developed using the ECL system according to the manufacturer's instructions. The signal density was analyzed using NIH Image J software and the relative protein level was calculated as the density ratio of the target protein to β-actin.

2.8. Chromatin immunoprecipitation–quantitative PCR (qCHIP)

qChIP assay was performed using SimpleChIP kit (Cell Signaling Technology) according to the manufacturer's protocols. Briefly, nuclei were prepared from cells crosslinked with 1% formaldehyde. Micrococcal nuclease was used to partially digest the chromatin, which was then sonicated to generate DNA/protein fragments of 150–900 base pairs (bps) in length. Upon incubating the digested chromatin with anti-PRMT1 (ab73246) antibody, anti-H4R3me2as (#39705, Active Motif, Carlsbad, CA, USA), or normal rabbit IgG (negative control; Cell Signaling Technology) at 4 °C overnight, the immune complexes were pulled down using ChIP-grade protein G magnetic beads. After eluting chromatin from the antibody/protein G magnetic beads, DNA was purified using the spin column provided with the kit and examined with qPCR analysis using ATF6 primer according to the qPCR manufacturer's protocols.

2.9. Luciferase reporter assay

The promoter sequences of mouse ATF6 gene was cloned into psiCHECK-2 luciferase reporter plasmid and transfected into sh-NC or sh-PRMT1 HK2 cells using Lipofectamine 2000 according to the manufacturer's instructions. Upon treating the cells with high glucose (30 mM) for 24 h, luciferase activity was detected using the Dual Luciferase Reporter Assay System (Promega, USA) according to the manufacturer's instructions.

2.10. Apoptosis assay by flow cytometry

To detect cellular apoptosis, HK2 cells upon different treatments were trypsinized, washed with PBS, and prepared into single-cell suspension. Then 5×10^5 HK2 cells were dual stained with 5 μL of FITC annexin V solution and 1 μL of propidium iodide (PI) solution provided with Dead Cell Apoptosis Kit (Thermo Fisher Scientific) at room temperature for 15 min, following the manufacturer's protocol, and detected by FACSCalibur flow machine (BD Biosciences).

2.11. Statistical analysis

All data were analyzed by SPSS 13.0 software and presented as mean ± SD from at least three independent experiments. All data were tested for and confirmed to present normal distribution using Shapiro-Wilk test. Differences between groups were assessed by one-way ANOVA with post-hoc Turkey test. $P \leq 0.05$ was considered statistically significant.

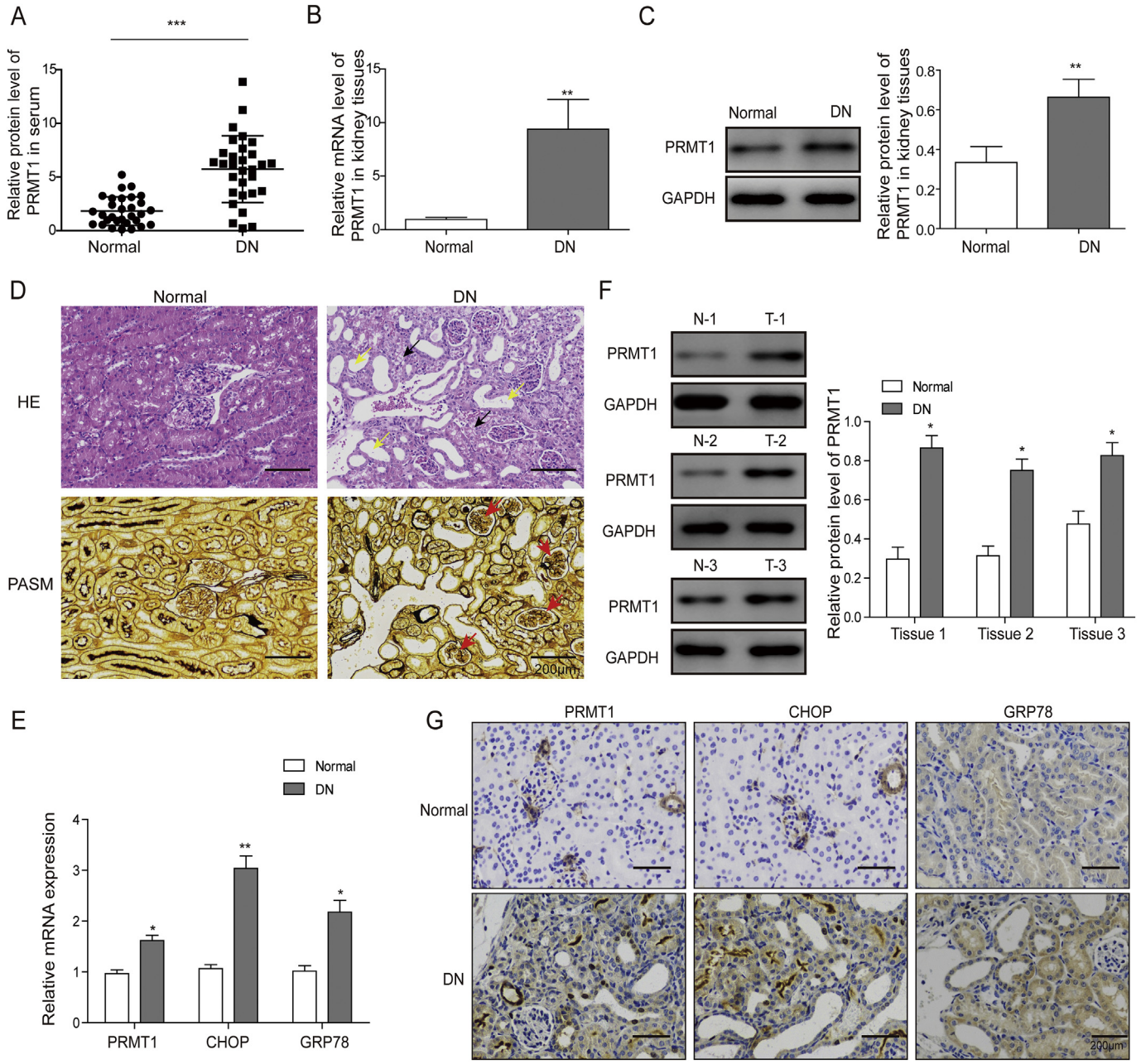

Fig. 1. PRMT1 is upregulated in patients with DN, in mice suffering DN, and is associated with elevated ER stress. A. Peripheral blood was collected from DN patients (DN; $n = 30$) and healthy individuals (Normal; n = 30). The serum level of PRMT1 was determined by ELISA and compared between the two groups. B. to D. Renal tissues were isolated from healthy individuals (normal) or DN patients. B. Total RNA was extracted from renal tissues and the steady-state mRNA level of PRMT1 were examined by RT-qPCR and compared between the two groups. C. The protein level of PRMT1 in renal tissues were examined by Western blot and compared between normal (n = 3) and DN patients ($n = 10$). GAPDH was determined as the internal control. D. HE staining (upper panels) and PASM staining (lower panels) revealed pathological changes typical of DN in patients, but not in normal individuals. E. to G. Renal tissues were isolated from normal or DN mice. E. Total RNA was extracted from renal tissues and the steady-state mRNA level of PRMT1, GRP78 and CHOP were examined by RT-qPCR and compared between normal and DN mice. F. The protein levels of PRMT1, GRP78 and CHOP in renal tissues were examined by Western blot and compared between normal and DN mice. G. The expressions of PRMT1, GRP78 and CHOP in renal tissues from normal and DN mice were detected by IHC. The data were expressed as mean ± s.d from three independent experiments. $^{*}P < 0.05$; $^{***} < 0.001$.

3. Results

3.1. PRMT1 is up-regulated in patients with DN or in mice suffering DN, and is associated with elevated ER stress

We first examined the level of PRMT1 in the serum from DN patients and also in renal tissues of mice suffering DN. When compared to the serum level of healthy individuals, PRMT1 was significantly up-regulated in DN patients (Fig. 1A). Furthermore, we found that the expression of PRMT1 (both the steady-state mRNA and protein level) was robustly up-regulated in DN patients, when compared to healthy individuals. In DN mice, we observed typical pathological alterations associated with DN, including segments of dilated renal tubules (yellow arrow) and vacuoles and granular degeneration of renal tubular epithelial cells (black arrows, from HE-stained samples), thickening of glomerular basement membrane (as indicated by positive PASM staining, red arrows, Fig. 1D). Similar to changes in DN patients, both the steady-state mRNA (Fig. 1E) and protein levels (Fig. 1F) of PRMT1

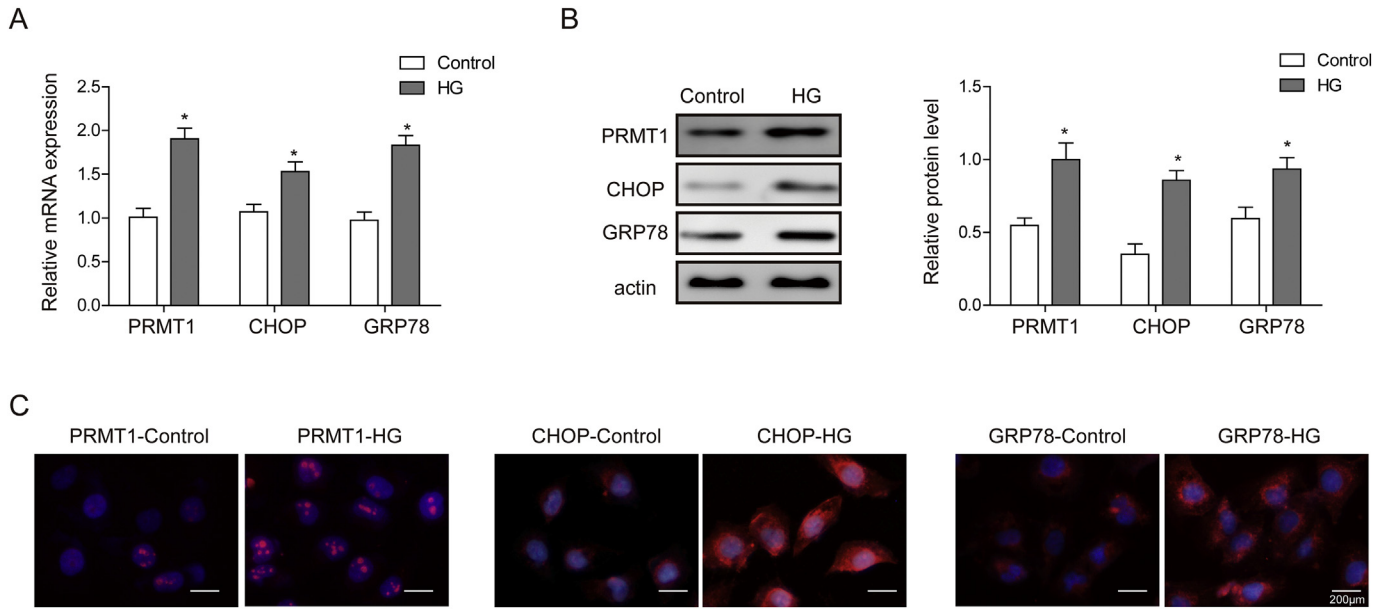

Fig. 2. High glucose induces both PRMT1 expression and ER stress in HK2 cells. HK2 cells were treated with high glucose (30 mM) for 48 h. A. The mRNA level of PRMT1 was examined by RT-qPCR and compared between control-treated and glucose-treated cells. B. The protein levels of PRMT1, GRP78, and CHOP were examined by Western blot and compared between indicated cells. C. 48 h after glucose treatment, respectively, the expressions of PRMT1, GRP78, and CHOP were examined by immunofluorescence (red signals). Blue signals represented DAPI-stained nuclei. The data were expressed as mean ± s.d. from three independent experiments. $^{*}P < 0.05$.

from renal tissues of DN mice were markedly higher than in tissues from control mice. Immunohistochemical analysis showed that PRMT1 was predominantly up-regulated in renal tissues of DN mice, concomitant with the higher expressions of GRP78 and CHOP, two well-demonstrated markers for ER stress [24] (Fig. 1E and G). Collectively, these data suggest that PRMT1 is up-regulated during DN development and concomitant with a higher level of ER stress.

3.2. High glucose induces both PRMT1 expression and ER stress in HK2 cells

To further explore the association between PRMT1 and ER stress and their functions and/or mechanisms in DN pathogenesis, we established an *in vitro* model where the normal PTEC cell line, HK2 cells were challenged with high glucose (30 mM). First, we examined the expressions of PRMT1, GRP78, and CHOP. We detected significant up-regulation of PRMT1 on both mRNA (Fig. 2A) and protein (Fig. 2B) levels. Concomitantly, the levels of GRP78 and CHOP were dramatically induced in high-glucose-challenged HK2 cells (Fig. 2A and B). Immunofluorescent staining confirmed the concomitant up-regulations of all three proteins (Fig. 2C), implying that PRMT1 may contribute to high glucose-induced ER stress in HK2 cells.

3.3. PRMT1 mediates high glucose-induced ER stress and cellular apoptosis in HK2 cells

To assess the functional significance of PRMT1 in high-glucose-induced ER stress in HK2 cells, we stably knocked down the expression of PRMT1 using shRNA-mediated gene silencing (sh-PRMT1). As shown in Fig. 3A, sh-PRMT1 potently reduced the expression of endogenous PRMT1, both on the mRNA (Fig. 3A) and protein levels (Fig. 3B) in non-treated HK2 cells or in those treated with high mannitol or high glucose, when compared to negative control shRNA (sh-NC). Of different treatments, high glucose, but not no-treatment or treatment with high mannitol, specifically up-regulated PRMT1, GPR78, and CHOP levels (both mRNA (Fig. 3A) and protein (Fig. 3B)) in sh-NC cells, but not in sh-PRMT1 cells, indicating that PRMT1 is essential for high-glucose-induced ER stress in these cells. Furthermore, we found that high glucose significantly induced apoptosis of sh-NC cells, which was significantly abolished in sh-PRMT1 cells (Fig. 3C), supporting that by controlling ER stress, down-regulating PRMT1 is sufficient to reduce apoptosis of HK2 cells induced by high glucose.

3.4. PRMT1 promotes high-glucose-induced ER stress by activating PERK and ATF6

Generally, ER stress is mediated by three major signaling transducers: PERK, IRE1α, and ATF6 [25]. When cloning the ATF6 promoter sequence into a luciferase reporter construct and transfecting the reporter construct into both sh-NC and sh-PRMT1 cells, we noticed the luciferase activity was significantly boosted in sh-NC cells treated with high glucose, but not in sh-PRMT1 cells upon the same treatment (Fig. 4A). Consistently, the ATF6 mRNA level was potently up-regulated in sh-NC cells treated with high glucose, but not in non-treated sh-NC cells or sh-PRMT1 cells treated with high-glucose (Fig. 4B). On the protein level, high glucose was sufficient to elevate the levels of p-PERK, p-eIF-2α, and ATF6, but not affecting that of p-IRE1. Knocking down PRMT1 abolished the glucose-induced up-regulations of p-PERK, p-eIF-2α and ATF6, without affecting that of p-IRE1 (Fig. 4C). Moreover, GSK2606414, a specific inhibitor for PERK, increased the inhibition effect of sh-PRMT1 on the expression of p-PERK, p-eIF-2α and ATF6, while AEBSF (a blocker for the cleavage of ATF6), only increased the inhibition effect of sh-PRMT1 on the expression of ATF6 (Fig. 4C). Since promoter methylation plays a role in regulating ATF6 level during ER stress [26] and PRMT1-mediated histone modification of H4R3me2as is linked to transcriptional activation [18], we intended to determine whether this modification is associated with the active transcription of ATF6 using qCHIP assay. As shown in Fig. 4D, both H4R3me2as and PRMT1 were abundantly detected within ATF6 promoter in sh-NC cells, but significantly reduced in sh-PRMT1 cells, indicating that PRMT1 facilitated the ATF6 transcriptional activation by enriching the H4R3me2as modification at the ATF6 promoter. All these data suggests that PRMT1 promotes glucose-induced ER stress by activating PERK and ATF6.

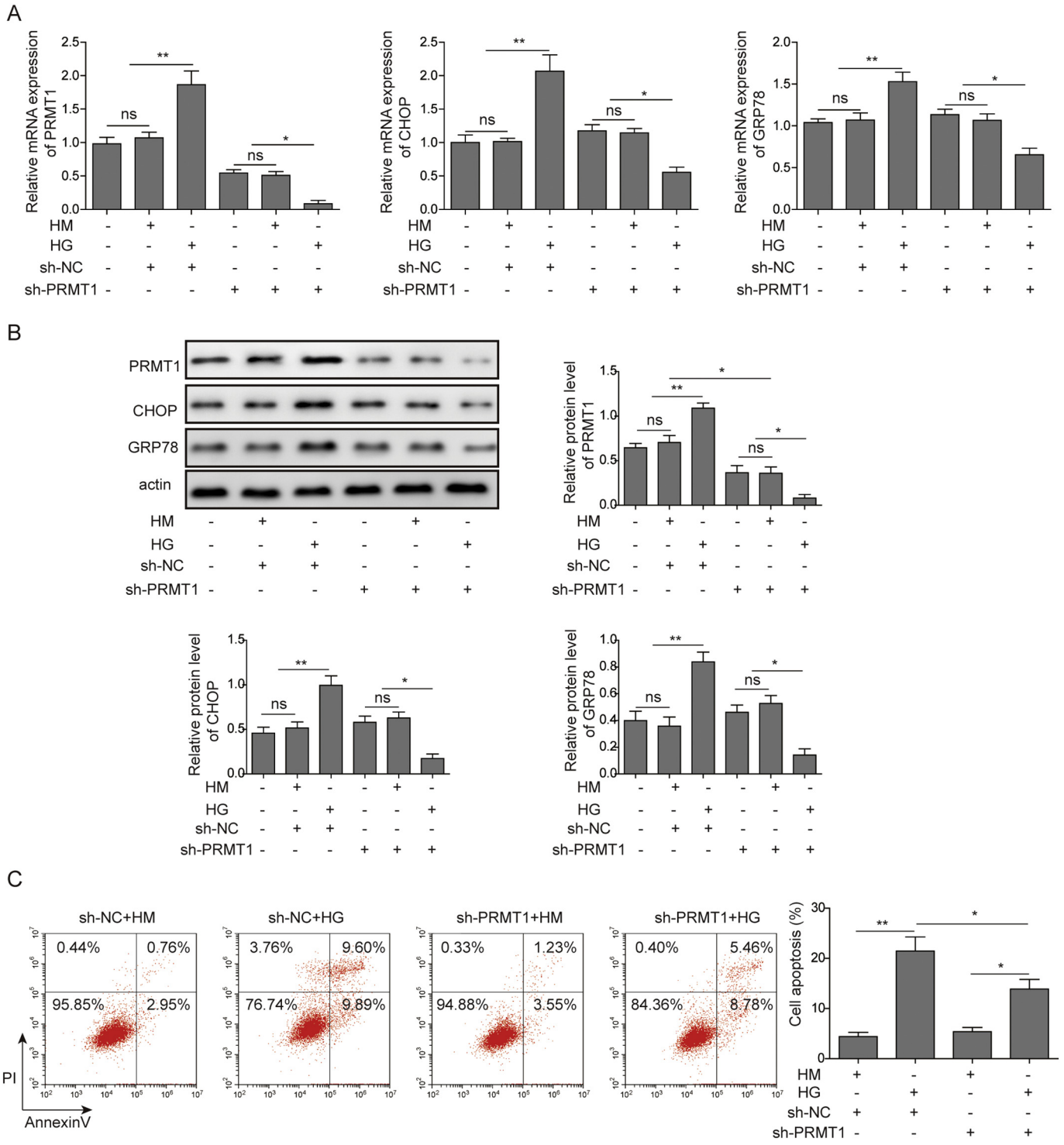

Fig. 3. PRMT1 mediates high glucose-induced ER stress and cellular apoptosis in HK2 cells. HK2 cells were stably transfected with either control (sh-NC) or PRMT1 shRNA (sh-PRMT1), and treated with either isotonic mannitol (5%) or high glucose (30 mM) for 24 h. A–B. The expression of PRMT1, GRP78, and CHOP on the mRNA and protein levels were examined by RT-qPCR (A) and Western blot (B), respectively. C. Apoptosis of indicated cells was examined by Annexin V-FITC and PI staining and represented by % of Annexin V-FITC$^+$PI$^+$ cells. The data were expressed as mean ± s.d. from three independent experiments. $^*P < 0.05$; $^{**} < 0.01$; $^{***} < 0.001$.

3.5. PRMT1 is sufficient and necessary for inducing EMT of HK2 cells

Several studies suggested a crosstalk between ER stress and EMT in different disease paradigms [11,13]. Considering that EMT plays a critical pathogenic role in DN development, we proposed that PRMT1, by inducing ER stress, may also promote EMT of PTECs and thus contribute to DN progression. To test this hypothesis, we applied both gain-of-function and loss-of-function approaches. Upon over-expressing PRMT1 in HK2 cells (Fig. 5A), we observed significant down-regulations of E-cadherin and β-catenin (two epithelial markers) and up-regulations of ZEB-1, fibronectin and α-SMA in HK2 cells depend on the culture time, when compared to cells expressing empty vectors

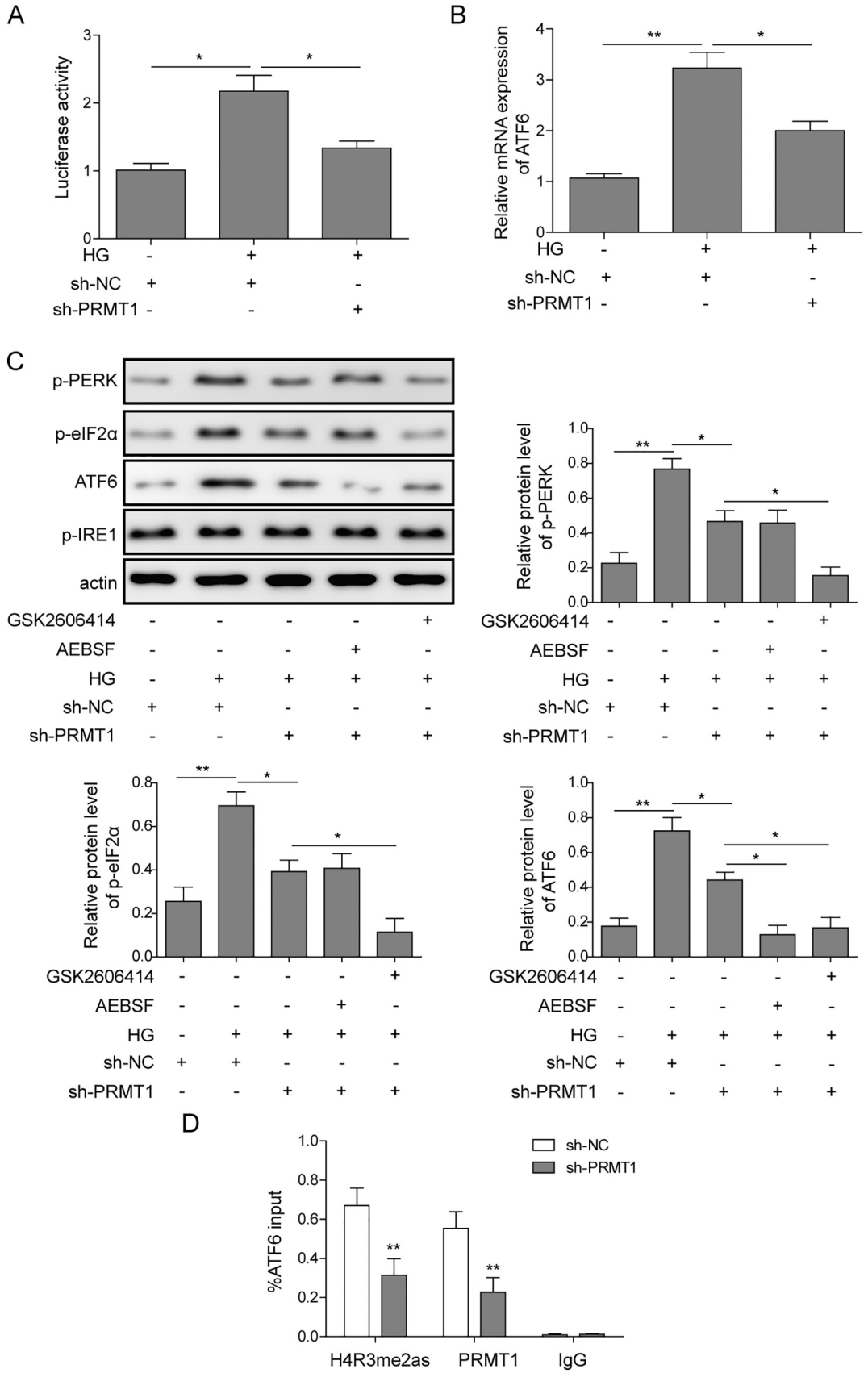

Fig. 4. PRMT1 induces ER stress by activating PERK and ATF6. A. The promoter sequence of mouse ATF6 gene was cloned into a luciferase reporter construct, which was then transfected into either sh-NC or sh-PRMT1 cells. Upon treating the cells with either vehicle or high glucose for 24 h, the luciferase activity was measured and compared between the groups. B. The mRNA level of endogenous ATF6 from indicated cells was determined by RT-qPCR. C. The protein levels of p-PERK, p-eIF2α, CHOP, cleaved ATF6, and p-IRE1 in indicated cells were examined by Western blot. β-actin was determined as the internal control. D. The abundance of H4R3me2as and PRMT1 within the promoter of ATF6 was determined using qChIP in sh-NC and sh-PRMT1 cells. IgG was used as a negative control. The data were expressed as mean ± s.d. from three independent experiments. $^{*}P < 0.05$; $^{**} < 0.01$; $^{***} < 0.001$.

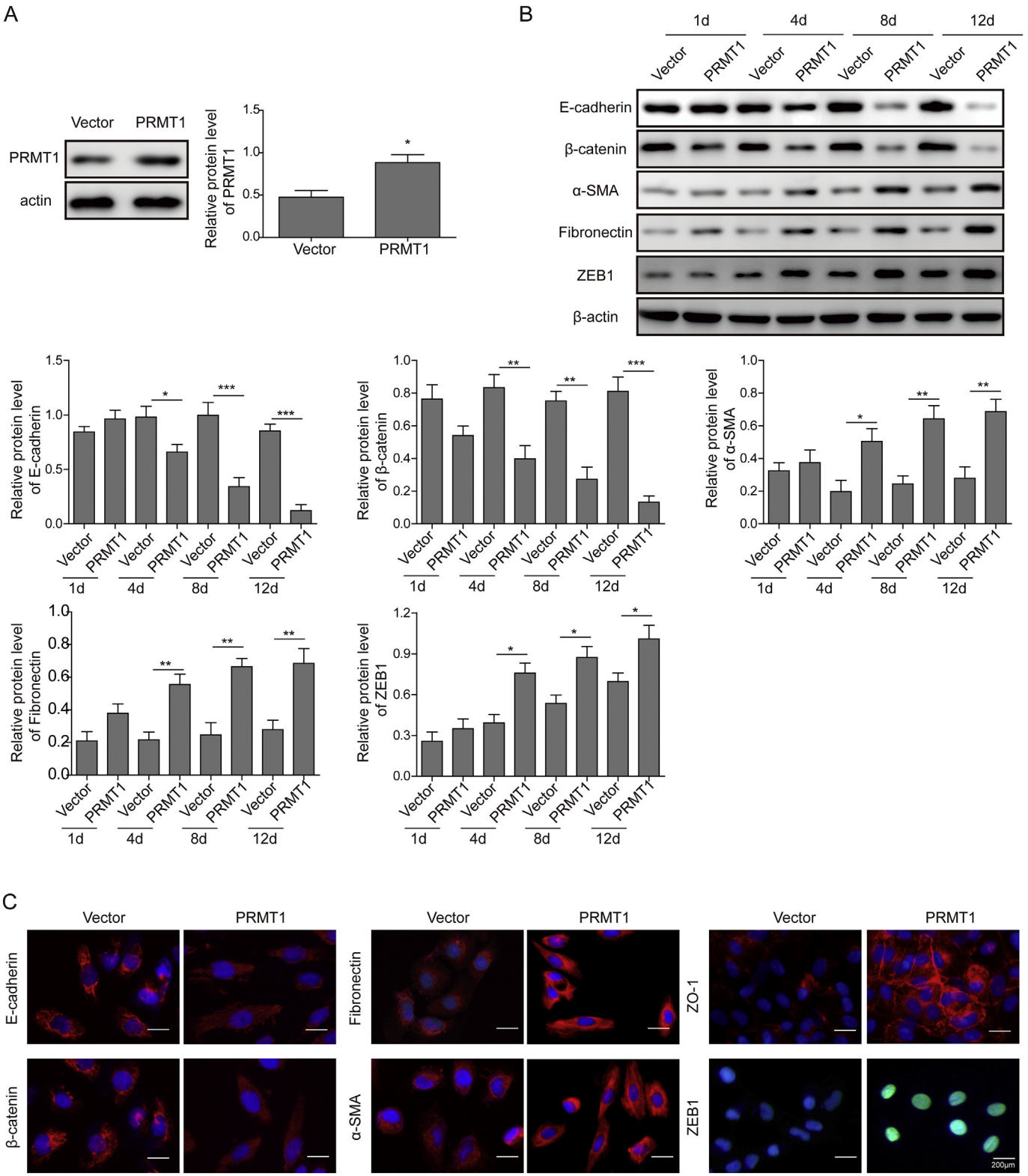

Fig. 5. Overexpression of PRMT1 induces EMT of HK2 cells. A. 48 h post-transfection of PRMT1 in HK2 cells. The expression of PRMT1 determined by Western blot. B. The protein levels of E-cadherin, β-catenin, fibronectin, α-SMA, and ZEB1 were determined by Western blot after transfection for 1d, 4d, 8d and 12d. β-actin was determined as the internal control. C. The expressions of E-cadherin, β-catenin, fibronectin, α-SMA, ZEB1, and ZO-1 in either control or PRMT1-overexpressing cells were examined by IF at 12d after transfection. The data were expressed as mean ± s.d. from three independent experiments. $^{*}P < 0.05$; $^{**} < 0.01$; $^{***} < 0.001$.

(Fig. 5B). Immunofluorescent staining also revealed the decreased expressions of E-cadherin and β-catenin, and the increased expressions of ZEB-1, ZO-1, fibronectin, and α-SMA induced by over-expressing PRMT1 in HK2 cells after 12 days post-transfection (Fig. 5C).

In response to high glucose, both the mRNA and protein levels of ZEB-1, ZO-1, fibronectin and α-SMA were elevated, while those of E-cadherin and β-catenin were reduced, suggesting that high glucose induced EMT in HK2 cells. When knocking down endogenous PRMT1,

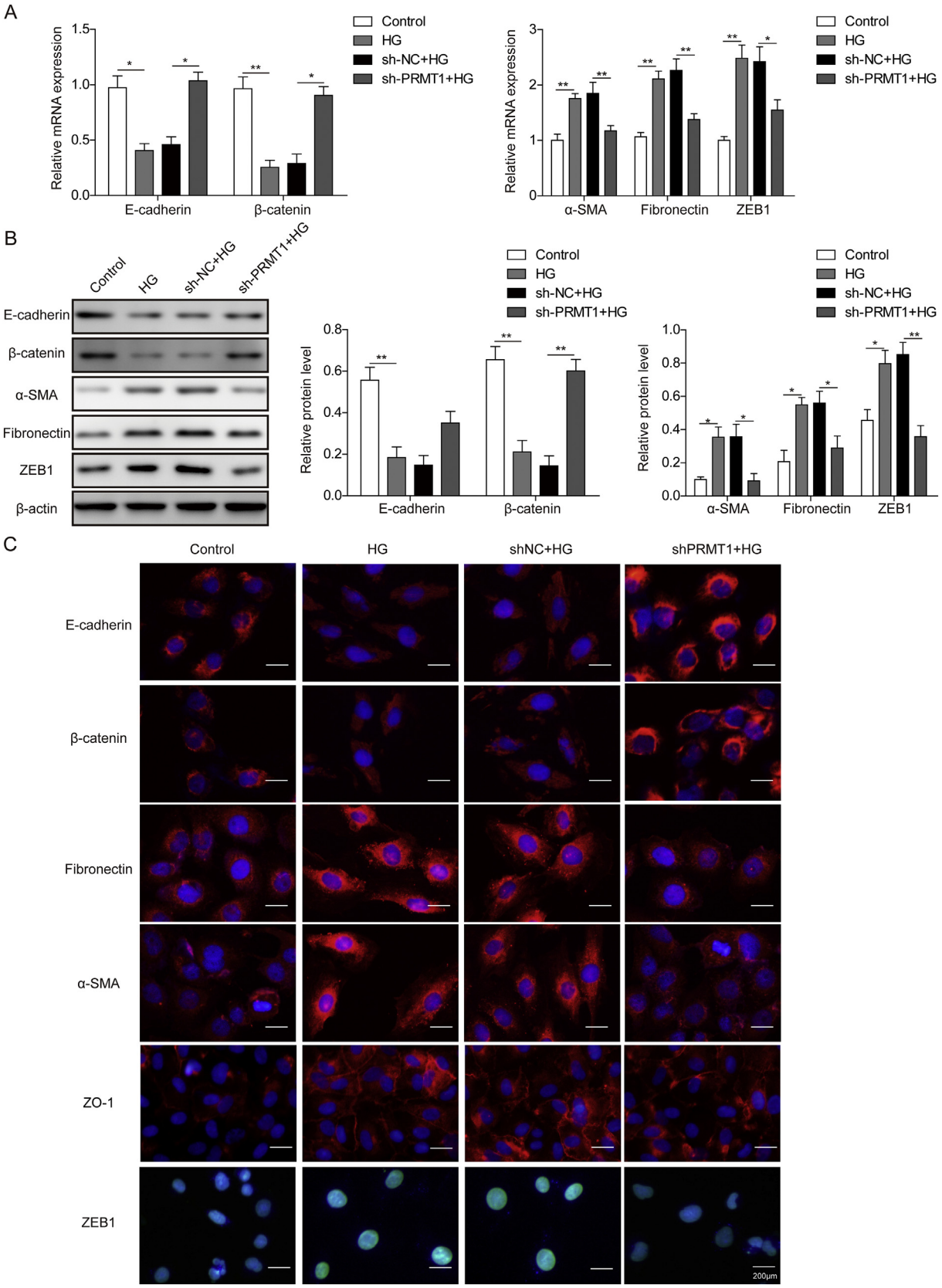

Fig. 6. Knockdown of PRMT1 inhibits high glucose-induced EMT of HK2 cells. sh-NC, or sh-PRMT1 HK2 cells were treated with either control or high glucose (30 mM) for 12 days. The expressions of E-cadherin, β-catenin, fibronectin, α-SMA, and ZEB1 were examined by RT-qPCR (A), Western blot (B), or IF (C), respectively. The data were expressed as mean ± s.d. from three independent experiments. $^{*}P < 0.05$; $^{**} < 0.01$.

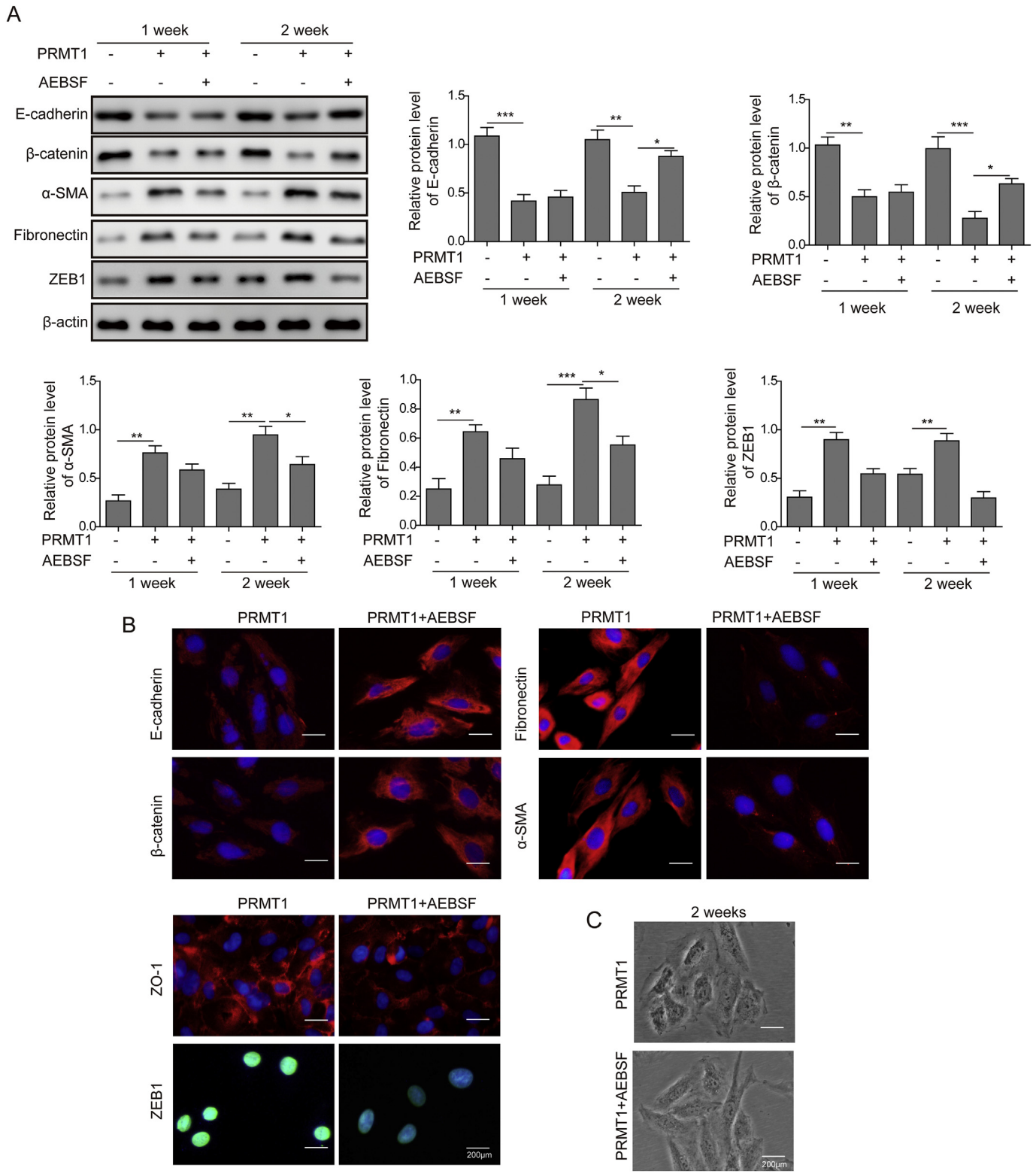

Fig. 7. ATF6 mediates PRMT1-induced EMT. PRMT1-overexpressing HK2 cells were treated without or with AEBSF (a specific ATF6 inhibitor) in serum-free medium for 30 min, followed by high glucose (30 mM) for a further 48 h, and repeat operation for future 1or 2 weeks. The expressions of E-cadherin, β-catenin, fibronectin, α-SMA, ZEB1, and ZO-1 in indicated cells were determined by Western blot (A) and IF (2 weeks, B), respectively. C. At two weeks after vehicle (PBS) or AEBSF treatment, the morphology of PRMT1-overexpressing cells was imaged under a light microscope. The data were expressed as mean ± s.d. from three independent experiments. *P < 0.05; ** < 0.01; *** < 0.001.

however, the high glucose-induced changes on the expressions of ZEB-1, ZO-1, fibronectin, α-SMA, E-cadherin, and β-catenin were significantly suppressed (Fig. 6A to C), indicating that PRMT1 is essential for mediating EMT in response to high glucose challenge.

3.6. ATF6 mediates PRMT1-induced EMT

Earlier findings that ATF6 mediated PRMT1-induced ER stress (Fig. 4) and PRMT1 essentially regulated EMT (Fig. 5), when combined with studies reporting the importance of ATF6 in regulating EMT [27,28], prompted us to examine the significance of ATF6 in PRMT1-mediated EMT. For this purpose, we treated PRMT1-overexpressing HK2 cells with AEBSF, the specific inhibitor for the cleavage of ATF6 and thus the transcriptions of ATF6 targets [29]. Consistent with earlier data (Fig. 5B), overexpressing PRMT1 significantly up-regulated ZEB-1, ZO-1, fibronectin and α-SMA, while down-regulated β-catenin and E-cadherin, and thus inducing EMT (Fig. 7A). Targeting ATF6 by AEBSF over a longer time period (specifically after two weeks) potently rescued PRMT1-induced down-regulation of β-catenin and E-cadherin, as well the up-regulation of ZEB-1, fibronectin and α-SMA (Fig. 7A), however, PERK inhibitor presented no further impacts on the expressions of PRMT1-regulated (Supplemental Fig. 1),suggesting that ATF6 is critical for controlling EMT induced by PRMT1. Immunofluorescent staining (Fig. 7B) on distinct EMT markers in cells after two weeks of indicated treatments confirmed the observation from Western blot. Consistently, PRMT1-overexpressing HK2 cells presented spindle-shaped mesenchymal phenotypes, while the treatment with AEBSF returned the cells to cuboidal-shaped epithelial morphology (Fig. 7C). Together, these findings suggest that targeting ATF6 with AEBSF was sufficient to reverse PRMT1-induced EMT.

4. Discussion

In this study, we demonstrated that the higher expression of PRMT1 is associated with DN development. Furthermore, we revealed novel pathogenic mechanisms by which PRMT1 contributes to DN development: 1) by activating PERK and ATF6, PRMT1 enhanced ER stress and contributed to the apoptosis of PTECs; 2) ATF6 was essential for PRMT1-induced EMT. Therefore, targeting PRMT1 may provide therapeutic benefits in the treatment of DN.

As the major organelle to synthesize new and degrade old proteins, ER homeostasis is critical for maintaining normal cell functions. In response to many diabetic attributes, such as hyperglycemia, proteinuria, AGEs, and free fatty acids (FFA), misfolded and unfolded proteins accumulated in renal cells, activating UPR *via* three major pathways: PERK, ATF6 and IRE1α, and initiating ER stress [30,31]. During the early phase, ER stress stimulates the degradation of misfolded proteins and attempts to restore homeostasis [32]. In the face of excessive UPR, however, ER stress proceeds to cell death, leads to cell and tissue injuries, and contributes to DN pathogenesis by activating multiple pro-apoptotic signals such as CHOP and TNF-related apoptosis-inducing ligand signaling [33,34]. During DN development, the impact of ER stress is ubiquitous, presenting in and affecting podocytes, mesangial cells, glomerular endothelial cells, and tubular epithelial cells [10]. Consistently, here we found that in renal tissues from DN mice, GRP78 and CHOP were ubiquitously up-regulated, indicating the widespread presence of ER stress. When focusing on PTECs, we showed that high glucose, but not isotonic mannitol, could up-regulate biomarkers for ER stress, suggesting the specificity of ER stress to diabetic milieu. Furthermore, we detected enhanced apoptosis of PTECs only to high glucose, but not to isotonic mannitol, supporting the importance of ER stress in damaging these cells during DN development.

Although the mechanisms for UPR and ER stress-mediated cell death have been well characterized [35,36], little is known on the upstream mediators that convey the diabetic signals to induce UPR and ER stress. In this study, we identified PRMT1 as a novel molecule controlling UPR and ER stress to a common diabetic attribute, high glucose. As a ubiquitously expressed protein methyltransferase, PRMT1 acts on a variety of substrates and modulates a diversity of biological processes, including regulating gene expressions, altering the localization of intracellular proteins, modifying protein-RNA interactions, mediating downstream signaling of different receptors, and repairing double-strand DNA break [14]. Functionally, PRMT1 plays an important pathogenic role in the development of cancers, muscular dystrophy, amyotrophic lateral sclerosis, diabetes, renal failure, and chronic pulmonary diseases [14]. In contrast, only a few studies began to reveal the link between PRMT1 and DN. Ojima et al. reported that AGEs induced PRMT1 expression in PTECs, which in turn generated asymmetric dimethylarginine (ADMA), an inhibitor for nitric oxide synthase, and promoting DN development [15]. Park et al. found that PRMT1 was essential for lipotoxicity-induced ER stress and apoptosis of mesangial cells [16]. Most recently, Zhu reported elevated expression of PRMT1 in renal podocytes from DN patients, where PRMT1 mediated both the apoptosis and ECM deposition in response to high glucose [17]. Comparing to these studies, the novelty for this study is multi-fold. First, we showed that PRMT1 level was higher not only in the renal tissue from DN mice, but also in the peripheral circulation of DN patients, indicating that the up-regulation of PRMT1, both locally and systematically, is associated with DN development. Second, when focusing on the PTEC cell line, HK2 cells, we found that high glucose could induce PRMT1 expression, which was concomitant with the activation of ER stress and the enhanced apoptosis in these cells, suggesting a correlation between PRMT1 up-regulation and ER stress and cellular apoptosis during DN development. Functionally, knocking down PRMT1 was sufficient to abolish ER stress (as evidenced by the non-response of ER stress markers GPR78 and CHOP to high glucose) and also reducing apoptosis, demonstrating the essential role of PRMT1. Third, mechanistically, the effects of PRMT1 on ER stress and cellular apoptosis were achieved through activating PERK and ATF6 since sh-PRMT1 annihilated the activation of both molecules, but not that of IRE1α. Furthermore, we showed that PRMT1-induced activation of ATF6 was achieved through the recruitment of H4R3me2as, a mechanism utilized by PRMT1 to up-regulate ZEB1 and stimulate EMT in breast cancer cells [18]. Collectively, these data provided novel insights into the pathogenic role of PRMT1 in DN development.

Besides stimulating apoptosis and leading to cellular injury, ER stress has been shown to activate EMT and contribute to pulmonary fibrosis [37,38]. Considering that tissue injury and responsive ECM accumulation are key pathogenic events for DN development, and EMT is an important mechanism leading to excessive ECM production, we examined the potential of PRMT1-mediated ER stress in EMT of PTECs. Both the gain-of-function and the loss-of-function approaches showed that PRMT1, through the activation of ATF6, was not only sufficient but also necessary for EMT of PTECs. Consistently, Zhu showed that PRMT1 also controlled EMT and ECM deposition from renal podocytes [17], suggesting that PRMT1 may deploy the same mechanisms in different renal compartments to promote DN development. Furthermore, although Iwano, et al. suggests EMT significantly contributed to the conversion from PTECs to myofibroblasts and thus DN pathogenesis [8], another study failed to recognize the importance of EMT in this process [39]. Instead, two recent studies suggested that EMT directly targets the functionality, repair, and regeneration of TECs, as well as TEC-sustained inflammation [40,41]. Therefore, this study suggests that the multiple effects of PRMT1 in PTECs may, instead of stimulating myofibroblast formation, directly contribute to DN development. Furthermore, by applying inhibitors for ATF6 and PERK, we demonstrated the specific importance of ATF6 in PRMT1-induced EMT, although both mediated PRMT1-induced ER stress.

Cumulative evidence suggests the beneficial effects of targeting ER stress in attenuating kidney damage in experimental models [42,43]. The novel findings that ATF6 and PERK significantly regulated PRMT1 activities in PTECs suggest that targeting ATF6 and/or PERK may

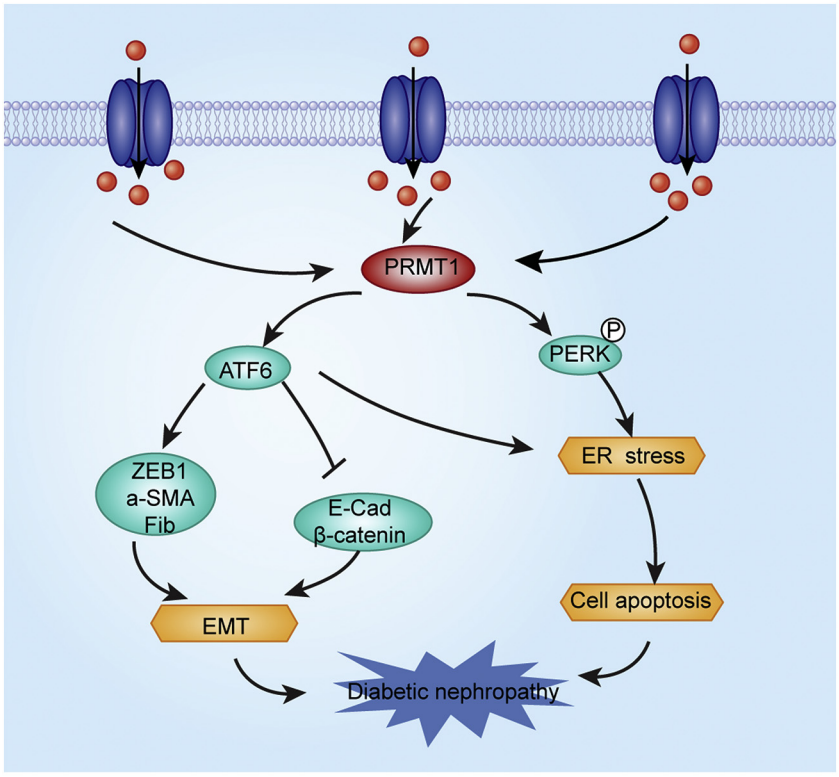

Fig. 8. A schematic diagram demonstrated how high gulose induces ER stress and EMT of HK-2 cells *via* PRMT.

alleviate DN-associated pathological changes. Particularly, since ATF6 mediates PRMT1-induced ER and EMT, while PERK only acts on the ER stress but not EMT, inhibitors for ATF6 signaling should be further explored in future studies in preclinical models of DN.

5. Conclusions

In summary, here we reported for the first time that PRMT1 essentially mediated ER stress in response to diabetic milieu, and further controlled ER stress-induced apoptosis and EMT in PTECs. The effects of PRMT1 in PTECs were achieved by activating PERK and ATF6 UPR pathways, and ATF6 essentially controlled PRMT1-induced EMT (A schematic diagram showing in Fig. 8). Therefore, inhibiting PRMT1 may simultaneously target cell injury, EMT, and fibrosis in PTECs, and thus benefit the treatment of DN.

Supplementary data to this article can be found online at https://doi.org/10.1016/j.bbadis.2019.06.001.

Transparency document

The Transparency document associated this article can be found, in online version.

Declaration of Competing Interest

The authors declare that they have no conflict of interest.

Acknowledgements

We would like to give our sincere gratitude to the reviewers for their constructive comments.

Funding

This work was supported by the National Natural Science Foundation of China, China (No.81870500), the Grant of Hunan Health Commission, China (No.B20180428), the Health and Family Planning Commission of Hunan Province, China (No.20180922), the Changde Municipal Science and Technology Bureau, China (No.2016KZ34), and the Research Grant of Traditional Chinese Medicine in Hunan, China (No.201826).

References

[1] V. Jha, G. Garcia-Garcia, K. Iseki, Z. Li, S. Naicker, B. Plattner, R. Saran, A.Y. Wang, C.W. Yang, Chronic kidney disease: global dimension and perspectives, Lancet. 382 (9888) (2013) 260–272.
[2] M. Narres, H. Claessen, S. Droste, T. Kvitkina, M. Koch, O. Kuss, A. Icks, The incidence of end-stage renal disease in the diabetic (compared to the non-diabetic) population: a systematic review, PLoS One 11 (1) (2016) e0147329.
[3] O. Gheith, N. Farouk, N. Nampoory, M.A. Halim, T. Al-Otaibi, Diabetic kidney disease: worldwide difference of prevalence and risk factors, J. Nephropharmacol. 5 (1) (2016) 49–56.
[4] T.W. Tervaert, A.L. Mooyaart, K. Amann, A.H. Cohen, H.T. Cook, C.B. Drachenberg, F. Ferrario, A.B. Fogo, M. Haas, E. de Heer, et al., Pathologic classification of diabetic nephropathy, J. Am. Soc. Nephrol. 21 (4) (2010) 556–563.
[5] C. Hu, L. Sun, L. Xiao, Y. Han, X. Fu, X. Xiong, X. Xu, Y. Liu, S. Yang, F. Liu, et al., Insights into the mechanisms involved in the expression and regulation of extracellular matrix proteins in diabetic nephropathy, Curr. Med. Chem. 22 (24) (2015) 2858–2870.
[6] E. Pedagogos, T. Hewitson, I. Fraser, K. Nicholls, G. Becker, Myofibroblasts and arteriolar sclerosis in human diabetic nephropathy, Am. J. Kidney Dis. 29 (6) (1997) 912–918.
[7] I. Loeffler, G. Wolf, Epithelial-to-mesenchymal transition in diabetic nephropathy: fact or fiction? Cells. 4 (4) (2015) 631–652.
[8] M. Iwano, D. Plieth, T.M. Danoff, C. Xue, H. Okada, E.G. Neilson, Evidence that fibroblasts derive from epithelium during tissue fibrosis, J. Clin. Invest. 110 (3) (2002) 341–350.
[9] K. Reidy, K. Susztak, Epithelial-mesenchymal transition and podocyte loss in diabetic kidney disease, Am. J. Kidney Dis. 54 (4) (2009) 590–593.
[10] Y. Fan, K. Lee, N. Wang, J.C. He, The role of endoplasmic reticulum stress in diabetic nephropathy, Curr. Diab. Rep. 17 (3) (2017) 17.
[11] Y.X. Feng, E.S. Sokol, C.A. Del Vecchio, S. Sanduja, J.H. Claessen, T.A. Proia, D.X. Jin, F. Reinhardt, H.L. Ploegh, Q. Wang, et al., Epithelial-to-mesenchymal transition activates PERK-eIF2alpha and sensitizes cells to endoplasmic reticulum stress, Cancer Discov. 4 (6) (2014) 702–715.
[12] P.P. Shah, T.V. Dupre, L.J. Siskind, L.J. Beverly, Common cytotoxic chemotherapeutics induce epithelial-mesenchymal transition (EMT) downstream of ER stress,

Oncotarget. 8 (14) (2017) 22625–22639.
[13] Q. Zhong, B. Zhou, D.K. Ann, P. Minoo, Y. Liu, A. Banfalvi, M.S. Krishnaveni, M. Dubourd, L. Demaio, B.C. Willis, et al., Role of endoplasmic reticulum stress in epithelial-mesenchymal transition of alveolar epithelial cells: effects of misfolded surfactant protein, Am. J. Respir. Cell Mol. Biol. 45 (3) (2011) 498–509.
[14] T.B. Nicholson, T. Chen, S. Richard, The physiological and pathophysiological role of PRMT1-mediated protein arginine methylation, Pharmacol. Res. 60 (6) (2009) 466–474.
[15] A. Ojima, Y. Ishibashi, T. Matsui, S. Maeda, Y. Nishino, M. Takeuchi, K. Fukami, S. Yamagishi, Glucagon-like peptide-1 receptor agonist inhibits asymmetric dimethylarginine generation in the kidney of streptozotocin-induced diabetic rats by blocking advanced glycation end product-induced protein arginine methyltranferase-1 expression, Am. J. Pathol. 182 (1) (2013) 132–141.
[16] M.J. Park, H.J. Han, D.I. Kim, Lipotoxicity-induced PRMT1 exacerbates mesangial cell apoptosis via endoplasmic reticulum stress, Int. J. Mol. Sci. 18 (7) (2017).
[17] Y. Zhu, PRMT1 mediates podocyte injury and glomerular fibrosis through phosphorylation of ERK pathway, Biochem. Biophys. Res. Commun. 495 (1) (2018) 828–838.
[18] Y. Gao, Y. Zhao, J. Zhang, Y. Lu, X. Liu, P. Geng, B. Huang, Y. Zhang, J. Lu, The dual function of PRMT1 in modulating epithelial-mesenchymal transition and cellular senescence in breast cancer cells through regulation of ZEB1, Sci. Rep. 6 (19874) (2016).
[19] B. Li, L. Liu, X. Li, L. Wu, miR-503 suppresses metastasis of hepatocellular carcinoma cell by targeting PRMT1, Biochem. Biophys. Res. Commun. 464 (4) (2015) 982–987.
[20] Y. Zhang, D. Wang, M. Zhang, H. Wei, Y. Lu, Y. Sun, M. Zhou, S. Gu, W. Feng, H. Wang, et al., Protein arginine methyltransferase 1 coordinates the epithelial-mesenchymal transition/proliferation dichotomy in gastric cancer cells, Exp. Cell Res. 362 (1) (2018) 43–50.
[21] D. Verzola, M.B. Bertolotto, B. Villaggio, L. Ottonello, F. Dallegri, F. Salvatore, V. Berruti, M.T. Gandolfo, G. Garibotto, G. Deferrari, Oxidative stress mediates apoptotic changes induced by hyperglycemia in human tubular kidney cells, J. Am. Soc. Nephrol. 15 (Suppl. 1) (2004) S85–S87.
[22] L. Xiao, X. Xu, F. Zhang, M. Wang, Y. Xu, D. Tang, J. Wang, Y. Qin, Y. Liu, C. Tang, et al., The mitochondria-targeted antioxidant MitoQ ameliorated tubular injury mediated by mitophagy in diabetic kidney disease via Nrf2/PINK1, Redox Biol. 11 (2017) 297–311.
[23] X. Rao, X. Huang, Z. Zhou, X. Lin, An improvement of the 2ˆ(-delta delta CT) method for quantitative real-time polymerase chain reaction data analysis, Biostat. Bioinform. Biomath. 3 (3) (2013) 71–85.
[24] Y.Z. Zheng, Z.G. Cao, X. Hu, Z.M. Shao, The endoplasmic reticulum stress markers GRP78 and CHOP predict disease-free survival and responsiveness to chemotherapy in breast cancer, Breast Cancer Res. Treat. 145 (2) (2014) 349–358.
[25] Z. Liu, Y. Lv, N. Zhao, G. Guan, J. Wang, Protein kinase R-like ER kinase and its role in endoplasmic reticulum stress-decided cell fate, Cell Death Dis. 6 (2015) e1822.
[26] H. Han, J. Hu, M.Y. Lau, M. Feng, L.M. Petrovic, C. Ji, Altered methylation and expression of ER-associated degradation factors in long-term alcohol and constitutive ER stress-induced murine hepatic tumors, Front. Genet. 4 (224) (2013).
[27] X. Shen, Y. Xue, Y. Si, Q. Wang, Z. Wang, J. Yuan, X. Zhang, The unfolded protein response potentiates epithelial-to-mesenchymal transition (EMT) of gastric cancer cells under severe hypoxic conditions, Med. Oncol. 32 (1) (2015) 447.
[28] X. Tang, X. Liang, M. Li, T. Guo, N. Duan, Y. Wang, G. Rong, L. Yang, S. Zhang, J. Zhang, ATF6 pathway of unfolded protein response mediates advanced oxidation protein product-induced hypertrophy and epithelial-to-mesenchymal transition in HK-2 cells, Mol. Cell. Biochem. 407 (1–2) (2015) 197–207.
[29] T. Okada, K. Haze, S. Nadanaka, H. Yoshida, N.G. Seidah, Y. Hirano, R. Sato, M. Negishi, K. Mori, A serine protease inhibitor prevents endoplasmic reticulum stress-induced cleavage but not transport of the membrane-bound transcription factor ATF6, J. Biol. Chem. 278 (33) (2003) 31024–31032.
[30] M.T. Lindenmeyer, M.P. Rastaldi, M. Ikehata, M.A. Neusser, M. Kretzler, C.D. Cohen, D. Schlondorff, Proteinuria and hyperglycemia induce endoplasmic reticulum stress, J. Am. Soc. Nephrol. 19 (11) (2008) 2225–2236.
[31] J. Sieber, M.T. Lindenmeyer, K. Kampe, K.N. Campbell, C.D. Cohen, H. Hopfer, P. Mundel, A.W. Jehle, Regulation of podocyte survival and endoplasmic reticulum stress by fatty acids, Am. J. Physiol. Ren. Physiol. 299 (4) (2010) F821–F829.
[32] A.V. Cybulsky, The intersecting roles of endoplasmic reticulum stress, ubiquitin-proteasome system, and autophagy in the pathogenesis of proteinuric kidney disease, Kidney Int. 84 (1) (2013) 25–33.
[33] E. Morse, J. Schroth, Y.H. You, D.P. Pizzo, S. Okada, S. Ramachandrarao, V. Vallon, K. Sharma, R. Cunard, TRB3 is stimulated in diabetic kidneys, regulated by the ER stress marker CHOP, and is a suppressor of podocyte MCP-1, Am. J. Physiol. Ren. Physiol. 299 (5) (2010) F965–F972.
[34] M.D. Sanchez-Nino, A. Benito-Martin, A. Ortiz, New paradigms in cell death in human diabetic nephropathy, Kidney Int. 78 (8) (2010) 737–744.
[35] R. Sano, J.C. Reed, ER stress-induced cell death mechanisms, Biochim. Biophys. Acta 1833 (12) (2013) 3460–3470.
[36] N. Sovolyova, S. Healy, A. Samali, S.E. Logue, Stressed to death - mechanisms of ER stress-induced cell death, Biol. Chem. 395 (1) (2014) 1–13.
[37] H. Tanjore, T.S. Blackwell, W.E. Lawson, Emerging evidence for endoplasmic reticulum stress in the pathogenesis of idiopathic pulmonary fibrosis, Am. J. Phys. Lung Cell. Mol. Phys. 302 (8) (2012) L721–L729.
[38] H. Tanjore, D.S. Cheng, A.L. Degryse, D.F. Zoz, R. Abdolrasulnia, W.E. Lawson, T.S. Blackwell, Alveolar epithelial cells undergo epithelial-to-mesenchymal transition in response to endoplasmic reticulum stress, J. Biol. Chem. 290 (6) (2015) 3277.
[39] V.S. LeBleu, G. Taduri, J. O'Connell, Y. Teng, V.G. Cooke, C. Woda, H. Sugimoto, R. Kalluri, Origin and function of myofibroblasts in kidney fibrosis, Nat. Med. 19 (8) (2013) 1047–1053.
[40] M.T. Grande, B. Sanchez-Laorden, C. Lopez-Blau, C.A. De Frutos, A. Boutet, M. Arevalo, R.G. Rowe, S.J. Weiss, J.M. Lopez-Novoa, M.A. Nieto, Snail1-induced partial epithelial-to-mesenchymal transition drives renal fibrosis in mice and can be targeted to reverse established disease, Nat. Med. 21 (9) (2015) 989–997.
[41] S. Lovisa, V.S. LeBleu, B. Tampe, H. Sugimoto, K. Vadnagara, J.L. Carstens, C.C. Wu, Y. Hagos, B.C. Burckhardt, T. Pentcheva-Hoang, et al., Epithelial-to-mesenchymal transition induces cell cycle arrest and parenchymal damage in renal fibrosis, Nat. Med. 21 (9) (2015) 998–1009.
[42] Z. Mohammed-Ali, C. Lu, M.K. Marway, R.E. Carlisle, K. Ask, D. Lukic, J.C. Krepinsky, J.G. Dickhout, Endoplasmic reticulum stress inhibition attenuates hypertensive chronic kidney disease through reduction in proteinuria, Sci. Rep. 7 (2017) 41572.
[43] T.W. Jung, K.M. Choi, Pharmacological modulators of endoplasmic reticulum stress in metabolic diseases, Int. J. Mol. Sci. 17 (2) (2016).